New quantum numbers in collision theory. V. Orientation of He $2\,^1P$ state by 80-eV electron impact

Chun-Woo Lee*
The James Franck Institute, The University of Chicago, 5640 South Ellis Avenue, Chicago, Illinois 60637
(Received 16 July 1987)

It is found that two simple dynamical relations can explain most observations of experiments on the orientation of the He $2\,^1P$ state induced by electron impact versus scattering angle in the process $e(80\text{ eV})+\text{He}\ 1\,^1S\rightarrow e+\text{He}\ 2\,^1P$. In particular, by utilizing these relations and with the help of new quantum numbers, we identified a formula that can account for more than 80% of the orientation at large angles, which contains only three dynamical parameters of the form $\text{Im}(S^\dagger S)$ and one other, namely, the differential cross section at 180° scattering.

I. INTRODUCTION

In this paper, new quantum numbers considered throughout this series (Refs. 1–4, which will be called papers I–IV hereafter) are applied to the process

$$e(80\text{ eV})+\text{He}\ 1\,^1S\rightarrow e+\text{He}\ 2\,^1P \quad (1)$$

for the identification of the dynamical parameters on which the observed orientation depends most sensitively. The orientation, discussed here, refers to the expectation value of the angular momentum operator for the He $2\,^1P$ state with respect to the electron scattering angle. Its measurement was pioneered by Kleinpoppen and his colleagues[5] by electron-photon coincidence experiments.

Though a lot of theoretical work has been done for the orientation for this system, and despite the fact that many aspects for the underlying dynamics are now understood, several important problems still remain[6] and more experimental and theoretical work is still coming out.[7]

One of the old problems associated with the orientation for process (1) is the prediction of the sign of orientation at small and large angles. Kohmoto and Fano[8] first pointed out the relation between the signs of the orientation and of the scattering potential, which was later more extensively perused by Hermann and Hertel.[9] In particular, the latter work pointed out that the sign of the orientation at forward scattering angles could be predicted rather easily from the quantum formulation and exactly coincides with that obtained from a simple classical grazing[10] or rolling-ball[11] model. However, the rigor of their result has often been suspected[12] because of the complicated sign behaviors of many apparently significant dynamical terms appearing in the theoretical orientation formulas. The present work resolves the controversy in this problem. The extension of this work to other processes and systems is thus recommended.

However, the main result of this work is in the identification of the dynamical parameters to which the orientation is most sensitive for the process (1) at large scattering angles. At large angles, Madison and Winter,[5,12] showed that the sign of orientation is independent of the charge of the projectile, in contrast to the forward scattering case. More recently, Madison, Csanak, and Cartwright[13] found an astonishing result; namely, that the $l=2$ partial wave plays the most significant role in determining the sign of the orientation at large scattering angles. However, Ref. 13 has several limitations. Firstly, it completely disregards the interference among incident and outgoing partial waves and their corresponding complex conjugate waves in the quantum formulas for the orientation. Secondly, it does not make clear the reason why such an $l=2$ partial wave plays a special role for the orientation at large angles. In this paper, we succeeded in giving an orientation formula with only three dynamical parameters of the form $\text{Im}(S^\dagger S)$ and one further parameter, namely the differential cross section at 180° scattering. This formula explains more than 80% of the orientation at large angles. Two dynamical relations, the simple angle dependence of inverse differential cross section and the short-collision delay-time condition, played the most prominent role in obtaining this formula. With this, we could explain most of the observations on orientation on the process (1). Also, the astonishing result of Ref. 13 is shown to originate from the short delay time in the collision.

In this study, we have only made a detailed analysis of the process (1). However, one of the greatest assets of this paper can be found in the fact that the dependency of two simple dynamical relations on impact energy, atomic excitation process, and so on, is well-known or can be easily studied. By utilizing this knowledge our analysis can easily be extrapolated to other processes. Attempts have been made to indicate the possible applicability of the results to other impact energies, atomic excitation processes, and atomic systems. More detailed analysis is called for in the future.

Section II discusses the problem of identifying significant dynamical parameters and the possible significance of new quantum numbers for this purpose. Section III discusses the harmonic expansion on which the later sections are based. Section IV identifies significant dynamical parameters of $\langle D_{b\theta}\rangle$ and $\langle L_y D_{b\theta}\rangle$ for the orientation for the process (1). Finally, a discussion is given in Sec. V.

II. SIGNIFICANT DYNAMICAL PARAMETERS AND NEW QUANTUM NUMBERS

The identification of dynamical parameters on which observations most sensitively depend requires adaptation

of theory whenever a theoretical formulation appropriate to a certain range of variables proves inadequate in a different range. For example, expansion in partial waves is adequate for a large scattering angle but proves inadequate, thus requiring a lot of partial waves, for a small scattering angle where the first Born approximation affords a simple and transparent treatment. This contrast was minimized in paper IV by analyzing dynamical parameters into contributions from the first Born approximation and those from alternative procedures. Extending the partial-wave analysis to small-angle scattering that is required for the analysis at large angles will then prove redundant since the contributions of high partial waves cancel out at large angles.

Another example of redundancy owing to an inadequacy of theoretical formulation emerges in the very structure of the orientation formula. The orientation of a target is defined as the expectation value of the target's angular momentum component orthogonal to the projectile's scattering plane, a value which depends on the scattering angle θ and will be indicated here by $\langle L_y \rangle_\theta$ (the expectation values of other components of angular momentum vanish because of symmetry[14]). Theory, however, calculates this value indirectly as the ratio

$$\langle L_y \rangle_\theta = \frac{\langle L_y D_{b\theta} \rangle}{\langle D_{b\theta} \rangle} , \tag{2}$$

where $D_{b\theta}$ denotes the response[15] of a projectile detector placed in the scattering plane at an angle θ from the direction of incidence (b stands for the final states of the projectile). The mean value $\langle D_{b\theta} \rangle$ is accordingly equal to the scattering cross section $d\sigma/d\Omega$, while $\langle L_y D_{b\theta} \rangle$ represents the expectation value of joint detection of the projectile at an angle θ and of the target angular momentum L_y. Redundancy occurs in (2) through the presence of $D_{b\theta}$ in both the numerator and denominator without canceling out in the ratio of mean values. Effective cancellation is nevertheless provided by a suitable approximation procedure as will be seen in Sec. IV. Identifying such redundancies and avoiding them by exploiting *symmetries other than those under space rotation* in the collision formulas (or other features of a process) have been a guideline of this series.

One such symmetry concerns the permutation P of a wave function and its complex conjugate, whose products occur in the analytical structure of observables. Single elements of such structures that are even or odd under P pertain generally to charge and current distributions,[16] respectively, whereas the full expressions of observables are of course invariant under P, as discussed in paper III (e.g., geometrical elements of differential cross section and orientation are, respectively, even and odd under P but their products with dynamical parameters are even). States of a space and their adjoints have been labeled by unprimed and primed symbols throughout this series. A second symmetry, which pertains strictly to geometrical parameters, relates to the permutations Q of initial- and final-state variables, i.e., to permutations of polarizers and analyzers or of the collimators for incident and scattered particles. Initial and final states of projectiles (or target) have been labeled by a (or A) and b (or B), respectively.

The parities under P and Q have been introduced in papers I and II. Their initial application was to replace the set of projectile orbital quantum numbers l_a, l_b, l'_a, and l'_b for the process (1) by the set with definite parities under P and Q

$$\begin{aligned} &\sigma=(l_a+l_b+l'_a+l'_b)/2, \quad P\sigma=\sigma, \quad Q\sigma=\sigma \\ &\tau=(l_a+l_b-l'_a-l'_b)/2, \quad P\tau=-\tau, \quad Q\tau=\tau \\ &\zeta=(l_a-l_b+l'_a-l'_b)/2, \quad P\zeta=\zeta, \quad Q\zeta=-\zeta \\ &\eta=(l_a-l_b-l'_a+l'_b)/2, \quad P\eta=-\eta, \quad Q\eta=-\eta \, . \end{aligned} \tag{3}$$

Here orbital quantum numbers l_a and l_b of the projectile before and after the collision differ in an inelastic process which transfers angular momentum to the target and label the columns and rows of the scattering matrix S, respectively. The quantum numbers l'_a and l'_b perform the same role for the Hermitian conjugate matrix $S^\dagger$ which multiplies S in the formulas of cross section and orientation. Summations over all these four quantum numbers occur because their values are not selectively prepared or measured.

The differential cross section and the orientation of process (1) were transcribed in the notation (3) and discussed in paper I. Paper II concerned the geometrical interpretation of the parameters (3) and the restrictions imposed on them by the behavior of $6j$ coefficients. As an important by-product of paper II, the physical basis for Kohmoto and Fano's conjecture[8] on a "generalized Landé g factor" was found to be provided by the Ponzano-Regge semiclassical theory of angular momentum.[3] This theory has proved very useful for identifying the classical rolling-ball-like structure in quantum formulas of Ref. 17.

We claim that measured observables depend more sensitively on dynamical parameters labeled by the symmetrical quantum numbers (3) rather than by orbital quantum numbers. The basis of this claim can be found, as discussed in paper III, in that dynamical parameters in these new quantum numbers are classified by more commonly observed characteristics of a system, i.e., by different charge distributions under P and by different propensities under Q. This claim is tested in this paper by examining the contributions to orientation for the process (1) from different values of $\{\sigma,\tau,\zeta,\eta\}$ beyond the parity analysis studied in papers I and II, demonstrating its power in *separating out* significant dynamical parameters.

III. HARMONIC EXPANSION

In this paper our discussion is restricted to the differential cross section and the orientation of the process (1). The zero value ($L_A=0$) of the initial orbital momentum of the target state for (1) yields $K_A=0$, i.e., a zero value of its multipole moments. The multipole moment transfers K_t from a projectile to a target; ($\mathbf{K}_t=\mathbf{k}_a-\mathbf{k}_b^*=\mathbf{K}_B-\mathbf{K}_A^*$) introduced in paper III is then given by 0 and 1 for the differential cross section ($K_B=0$)

and the orientation ($K_B=1$), respectively. This in turn restricts the relevant multipole moments k_a and k_b of the projectile through the relation

$$1 \geq K_t \geq |k_a - k_b| \ . \tag{4}$$

The parity conditions $l_a+l_a'+k_a=$even, $l_b+l_b'+k_b=$even, and the parity conservation relation $L_A+l_a=L_B+l_b$ holding for the scattering matrix $(L_B M_B l_b m_b | S | L_A M_A l_a m_a)$ for the process (1) allow only even values of $|k_a-k_b|$. This, combined with (4), yields $k_a=k_b$ for both the differential cross section and the orientation expressions of process (1).[18] We set then, in the following:

$$k_a=k_b=k \ . \tag{5}$$

On this basis we may introduce harmonic expansions of the expectation values of the operators in the orientation formula (2) in terms of the Legendre functions $P_k(\cos\theta)$ and the associated Legendre functions $P_{k1}(\cos\theta)$

$$\begin{aligned} \langle D_{b\theta}\rangle &= \sum_k D_k P_k(\cos\theta) \ , \\ \langle L_y D_{b\theta}\rangle &= \sum_k N_k P_{k1}(\cos\theta) \ . \\ \langle L_y\rangle_\theta &= \sum_k L_k P_{k1}(\cos\theta) \ . \end{aligned} \tag{6}$$

Our study of the dependence of cross section and orientation on the quantum numbers $\{\sigma,\tau,\zeta,\eta\}$ will accordingly deal with the dependence of the harmonic coefficients D_k, N_k, and L_k on these indices. [We also note that both angular momentum transfer quantum numbers j_t and j_t' equal 1 ($=L_B$). This circumstance, together with (5), implies that the permutations P and Q considered generally in paper III have no effect on the indices $\{j_t,j_t',k_a,k_b\}$; only their influence on $\{l_a,l_b,l_a',l_b'\}\equiv\{\sigma,\tau,\zeta,\eta\}$ is accordingly relevant.]

In our study of the relation between observables and the dynamical parameters $S^\dagger S$, the harmonic expansion (6) plays the same role as the partial-wave expansion does in the analysis of scattering wave functions. A characteristic feature of the coefficients D_k,N_k,L_k in (6) at intermediate energies is that the expressions of $\langle D_{b\theta}\rangle$ and $\langle L_y D_{b\theta}\rangle$ contain large numbers of significant terms (recalling the uncertainty relation of θ and k), but the expansion of $\langle L_y\rangle_\theta$ does not. An understanding of this phenomenon is important for our analysis.

The phenomenon will be illustrated by the plots of D_k,N_k,L_k calculated by a distorted-wave Born procedure (DWBA). This type of procedure has proved successful in earlier calculations of process (1).[19] Only the first two or three coefficients L_k have appreciable values in contrast to the distributions of D_k and N_k. The latter distributions reflect primarily the large forward peak of $\langle D_{b\theta}\rangle$, which originates from dipole transitions of an atom produced at long ranges r by an interaction proportional to $1/r^2$. This peak effectively cancels in the ratio $\langle L_y D_{b\theta}\rangle/\langle D_{b\theta}\rangle$ of Eq. (2) even though $D_{b\theta}$ is averaged separately in the numerator and denominator. This remarkable cancellation could be understood by noticing that the reciprocal of the differential cross section $\langle D_{b\theta}\rangle$ is nearly proportional to $1-\cos\theta$ for the process (1),[20] which vanishes at $\theta=0$, as shown in Fig. 1. A more accurate and general application of this circumstance will be described in Sec. IV A.

IV. DEPENDENCE OF L_k ON DYNAMICAL PARAMETERS

Contributions to observables from terms with different quantum numbers have been sorted out in paper I by reorganizing the multiple sums over projectile orbitals,

$$\sum_{\sigma,\tau,\zeta,\eta} = \left[\sum_{(\sigma-k)/2=0}^{\infty} \sum_{(\tau+k-1)/2=0}^{k-1} \sum_{\eta=\pm1} \right]_{\zeta=0} + \left[\sum_{(\sigma-\tau-1)/2=0}^{\infty} \sum_{(\tau+k)/2=0}^{k} \sum_{\zeta=\pm1} \right]_{\eta=0} . \tag{7}$$

This operation was applied specifically to the harmonic analysis (6) of $\langle D_{b\theta}\rangle$ and $\langle L_y D_{b\theta}\rangle$. Its extension to the analysis of $\langle L_y\rangle_\theta$ would be straightforward if $\langle L_y\rangle_\theta$ were directly proportional to $\langle L_y D_{b\theta}\rangle$ but is complicated by its *nonlinear* dependence on $\langle D_{b\theta}\rangle$. This complication will be analyzed here.

Recall also that the ultimate aim of this work is to extract information on the dynamical parameters in Eq. (31) of paper III,

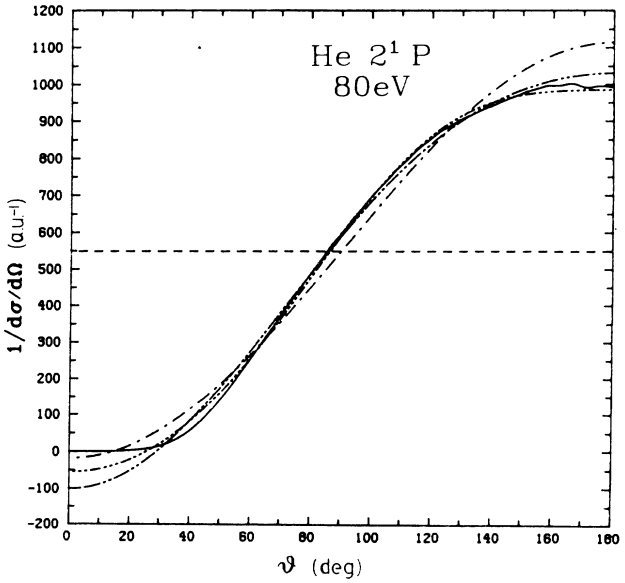

FIG. 1. Inverse of the DWBA differential cross section for process (1) at 80 eV and its truncated expansions in $P_k(\cos\theta)$ vs scattering angle: ——, total; — — —, truncated after the first term; —·—, after the second term; —··—, after the third term; — · · · —, after the fourth term.

$$[S^{\dagger}(j_t')S(j_t)]_{\sigma,\tau,\xi,\eta} + (-1)^{j_t+j_t'+K_t}[S^{\dagger}(j_t')S(j_t)]_{\sigma,\tau,-\xi,-\eta} \cdot \quad (8)$$

The real and imaginary parts of these parameters occur, respectively, in the expansions of $\langle D_{b\theta}\rangle$ and of $\langle L_y D_{b\theta}\rangle$, for process (1), according to Eq. (29) of paper III. They are *note quite independent,* being related by dispersion relation integrals[21] extended over the whole energy spectrum, but are *practically independent* in observations within a *limited* range of collision energies. This assertion forms the basis of the separate treatments of dynamical parameters of $\langle D_{b\theta}\rangle$ and $\langle L_y D_{b\theta}\rangle$ for the analysis of orientation in Secs. IV A and IV B.

A. L_k and dynamical parameters of $\langle D_{b\theta}\rangle$

Two alternative approaches will be followed to make explicit the dependence of the harmonic coefficients L_k on the dynamical parameters of $\langle D_{b\theta}\rangle$ in the denominator of (2).

(a) Multiply (2) by $\langle D_{b\theta}\rangle$ and then project the equation onto each harmonic $P_{k1}(\cos\theta)$. This results in the linear system

$$\sum_{k'} U_{kk'}L_{k'} = C_k N_k \ , \quad (9)$$

whose matrix

$$U_{kk'} = \int_{-1}^{1} \langle D_{b\theta}\rangle P_{k1}(\cos\theta)P_{k'1}(\cos\theta)d(\cos\theta) = \sum_{k''} D_{k''} \begin{bmatrix} k & k' & k'' \\ 0 & 0 & 0 \end{bmatrix}^2 [k(k+1)+k'(k'+1)-k''(k''+1)] = \sum_{k''} D_{k''} \begin{bmatrix} k & k' & k'' \\ 0 & 0 & 0 \end{bmatrix}^2 2\mathbf{k}\cdot\mathbf{k}' \quad (10)$$

contains the dynamical parameters of $\langle D_{b\theta}\rangle$, while

$$C_k = \frac{2k(k+1)}{2k+1} \quad (11)$$

is the normalization integral of $P_{k1}(\cos\theta)$.

(b) Project the equation (2) directly onto $P_{k1}(\cos\theta)$ to obtain the solution of (9)

$$L_k = \sum_{k'} (U^{-1})_{kk'}C_{k'}N_{k'} \ , \quad (12)$$

in terms of the reciprocal matrix U^{-1} represented by an integral over the reciprocal $\langle D_{b\theta}\rangle^{-1}$,

$$(U^{-1})_{kk'} = (C_k C_{k'})^{-1} \int_{-1}^{1} \langle D_{b\theta}\rangle^{-1} P_{k1}(\cos\theta)P_{k'1} \times (\cos\theta)d(\cos\theta) \ . \quad (13)$$

Equation (12) proves more effective than (9), not only because it yields L_k directly, but especially because the matrix U^{-1} turns out to be approximately tridiagonal, reflecting the simple dependence of $\langle D_{b\theta}\rangle^{-1}$ on θ indicated in Sec. II. An approximate analytic expression of U^{-1} is given here; a study of U itself and of its inversion is given in Appendix B.

The analytic representation of $\langle D_{b\theta}\rangle^{-1}$ as proportional to $1-\cos\theta$ takes the form[20] (see Fig. 1 and Table I)

$$\langle D_{b\theta}\rangle^{-1} \approx \frac{1-\cos\theta}{2\langle D_{b\theta}\rangle_{\theta=\pi}} \ . \quad (14)$$

TABLE I. Coefficients D_k of $P_k(\cos\theta)$ for the expansion of $\langle D_{b\theta}\rangle$ for the process (1).

k	D_k (a.u.)
0	−544.8
1	562.3
2	82.6
3	−45.6
4	33.0
5	20.0

This formula condenses *all relevant dynamical characteristics* of a collision of interest in the simple value of $\langle D_{b\theta}\rangle$ for 180° scattering. This value depends presumably on the contributions of only a few partial waves in the expansion of the projectile wave function. Its use implies accordingly that the factor $1/\langle D_{b\theta}\rangle$ contributes little dynamical information to the orientation $\langle L_y\rangle_\theta$. Using (14) in the integral expression (13) shows that the matrix U^{-1} is almost tridiagonal with matrix elements

$$(U^{-1})_{k,k} \approx \frac{1}{2C_k\langle D_{b\pi}\rangle} \ ,$$
$$(U^{-1})_{k,k-1} \approx -\frac{k-1}{2k-1}(U^{-1})_{k-1,k-1} \ , \quad (15)$$
$$(U^{-1})_{k,k+1} \approx -\frac{k+2}{2k+3}(U^{-1})_{k+1,k+1} \ .$$

The values of $(U^{-1})_{11}$ and $(U^{-1})_{22}$ calculated by (15) are 3.36 and 1.87 for the process (1) at 80 eV, while their exact values are 3.41 and 1.78, respectively. The error of Eq. (15) for these significant matrix elements is thus less than 5%.

Returning now to the expression (12) of the harmonic coefficients of the orientation L_k, we note that these coefficients depend explicitly and approximately *linearly* only on the dynamical parameters in the expression $N_k(\sigma,\tau,\xi,\eta)$ given in Eq. (16) of paper I. The factor $\langle D_{b\theta}\rangle^{-1}$ of $\langle L_y\rangle_\theta$ has a twofold influence on each L_k: (a) it normalizes L_k through the value of $1/\langle D_{b\pi}\rangle$, and (b) it averages over each group of three coefficients $N_{k'}$, as indicated by

$$\sum_{k'} (U^{-1})_{k,k'}C_{k'}N_{k'} \approx \frac{1}{2\langle D_{b\pi}\rangle} \left[N_k - \frac{k-1}{2k-1}N_{k-1} - \frac{k+2}{2k+3}N_{k+1} \right] . \quad (16)$$

The values of L_k calculated by the approximate (16) and the exact values calculated from (9) or (12) without making use of (14) and (15) are compared in Table II. From Table II, we see that the inaccuracy of Eq. (16) is less than 7% for $L_1(\zeta=0)$ and $L_2(\zeta=0)$ but as large as 37% and 57% for $L_1(\eta=0)$ and $L_2(\eta=0)$, respectively. However, even for the latter, Eq. (16) gives the correct sign of orientation and thus may be used for a qualitative purpose. On the other hand, (16) is good for both qualitative and quantitative purpose for $L_k(\zeta=0)$, i.e., at large angles, as will be evident in Sec. IV B). Notice that the sum of the three coefficients of N_k in the large parentheses vanishes to $O(1/k^2)$. This approximate cancellation will prove important in Sec. IV. It also reduces greatly the computation time in the alternative calculation of U^{-1} by the method of Appendix B.

B. L_k and dynamical parameters of $\langle L_y/D_{b\theta}\rangle$

Observed orientation curves versus scattering angles of the projectile electron for the system (1) show a remarkably simple shape and resemble a sine curve. This indicates that only a few coefficients are needed for the expansion of orientation in terms of P_{k1}. The coefficients L_k of the harmonic expansion of the orientation for process (1) at 80 eV are plotted as a histrogram in Fig. 2. These coefficients have been obtained from the formulas of paper I using an input data basically the same scattering matrix elements calculated by DWBA of Ref. 19. All the other data provided in this paper derive from the same source.

Two main features are apparent in Fig. 2: (a) the very rapid convergence to zero of the coefficient L_k as k increases, and (b) the alternation in sign of the largest coefficients L_1 and L_2. The principal source for the rapid convergence of L_k derives from the cancellation of the three coefficients of N_k in (16), which becomes rapidly more effective with increasing k. The effectiveness of this cancellation presupposes a rather smooth dependence of N_k itself on k, which is illustrated by the joint plot of D_k, N_k, L_k in Fig. 3. An additional factor contributing to the convergence of L_k will be discussed in Sec. V. All of the following analyses rely on or utilize this rapid convergence of L_k.

The remaining analysis of this paper centers on the contributions to L_k, in Eq. (16), from terms of the N_k with different sets of quantum numbers $\{\sigma,\tau,\zeta,\eta\}$ because the influence of the denominator $\langle D_{b\theta}\rangle$ in Eq. (2) has already been taken into account through the structure of (16).

The contributions of different $\{\sigma,\tau,\zeta,\eta\}$ with $\eta=0$ (i.e., $\zeta=\pm1$) and with $\zeta=0$ ($\eta=\pm1$) are antisymmetric under the permutation Q of projectile preparation and detection, thus reflecting the influence of the propensity rule discussed in Sec. V of paper III. As discussed in paper II, terms with $\eta=0$ are classically allowed and most important to forward scattering, while those with $\zeta=0$ are classically forbidden and will be shown to be important to orientation at back scattering angles. The contributions from different ranges of σ correspond to large and small impact parameters, and those from different τ stem from interferences between larger and smaller orbital momenta of the projectile. Most contributions of larger τ accrue from the first born contributions. These properties of the new quantum numbers will be utilized directly in Secs. IV B 1–IV B 4 in order to identify the most significant dynamical parameters.

1. *Short collision delay time and the dominance of $\zeta=0$ at large angles*

Figure 4 shows $\langle L_y\rangle_\theta$ subdivided into the separate contributions from coefficients $N_k(\sigma,\tau,\zeta,\eta)$ with $\eta=0$ and with $\zeta=0$. The y axis in Fig. 4 is chosen parallel to $\hat{p}_b\times\hat{p}_a$ here, inverted in sign from another convention.[6] Note how the $\eta=0$ curve converges to zero at $\theta>90°$ and that for $\zeta=0$ remains near zero at smaller angles.

The prevalence of $\eta=0$ contributions to $\langle L_y\rangle_\theta$ at small angles parallels the prevalence of $\langle L_y D_{b\theta}\rangle$ in that range, which derives in turn from the large values and the uniform sign of $\sum_\zeta N_k(\sigma,\tau,\zeta,0)$ for all values of σ and τ. The same circumstance causes $\langle L_y D_{b\theta}\rangle$ to converge to zero at $\theta>90°$, where the sign of $P_{k1}(\cos\theta)$ alternates for even and odd values of k.

The predominance in magnitude of $\eta=0$ components to N_k (as well as to D_k) has been introduced in paper II with regard to the magnitude of their $6j$ coefficients. $6j$ coefficients belong mostly to a classically forbidden range for $\eta=0$ components, while belonging to a classically allowed range for $\zeta=0$ components. This predominance is enhanced when the magnitudes of the dynamical parameters are also included, as considered in paper III in connection with the propensity rules. That is, a (propensity favored-favored)–(propensity unfavored-unfavored) combination takes place for the dynamical parameters $S^\dagger S(\zeta=1)-S^\dagger S(\zeta=-1)$ with $\eta=0$ components, while a (propensity favored-unfavored)–(propensity unfavored-favored) combination takes place for the dynamical parameters with $\zeta=0$ components. The numerical values of N_k and D_k for $\eta=0$ and $\zeta=0$ components shown in Table III confirm the dominance of $\eta=0$ components. The influence of the predominance of $\eta=0$ components on the sign of orientation at small angles will be touched only lightly in Sec. IV B 4 in this paper (for more details, see Ref. 17). Here we want to pay more attention to how small-ζ components can dominate the orientation at large

TABLE II. Accuracy of the approximate formula (16) for the process (1).

Components	L_1 from (16)	L_1 (exact)	Error (%)	L_2 from (16)	L_2 (exact)	Error (%)
$\zeta=0$	0.630	0.677	7	−0.206	−0.186	2
$\eta=0$	−0.787	−0.495	37	−0.647	−0.274	57

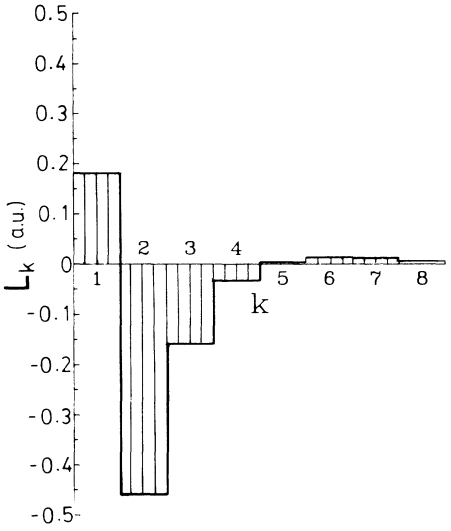

FIG. 2. Histogram of harmonic coefficients of the orientation for process (1) at 80 eV.

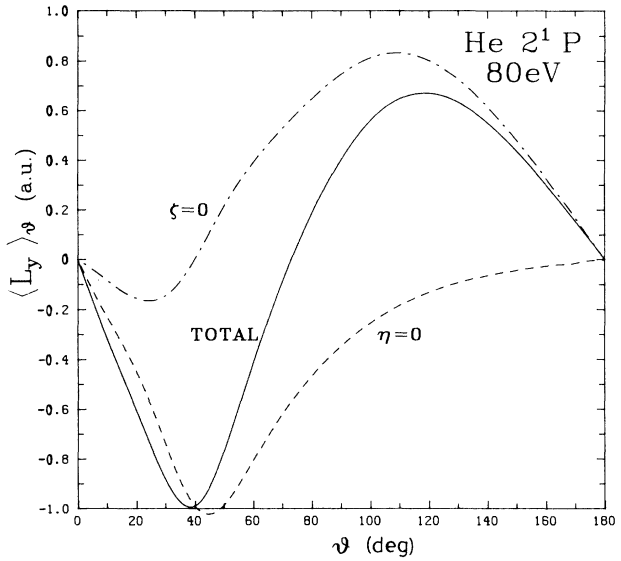

FIG. 4. Components $\eta=0$ and $\zeta=0$ of the orientation $\langle L_y \rangle_\theta$ as for Fig. 2.

angles.

Inspection of Table III shows that N_1 is abnormally small compared to other N_k for $\zeta=0$, while all N_k coefficients vary smoothly as a function of k for $\eta=0$. This derives from the short-collision delay-time condition holding for the process (1), as we proceed to show. Consider the imaginary parts of dynamical paramters (8) for N_k,

$$\begin{aligned}\mathrm{Im}[S^\dagger(j_t)S(j_t)]_{\sigma,\tau,\zeta,\eta}-\mathrm{Im}[S^\dagger(j_t)S(j_t)]_{\sigma,\tau,-\zeta,-\eta}\\ =S^\dagger(j_t)S(j_t)\,|_{\sigma,\tau,\zeta,\eta}\sin[\phi(l_a,l_b)-\phi(l_a',l_b')]\\ -|\,S^\dagger(j_t)S(j_t)\,|_{\sigma,\tau,-\zeta,-\eta}\sin[\phi(l_b,l_a)-\phi(l_b',l_a')]\ ,\end{aligned} \tag{17}$$

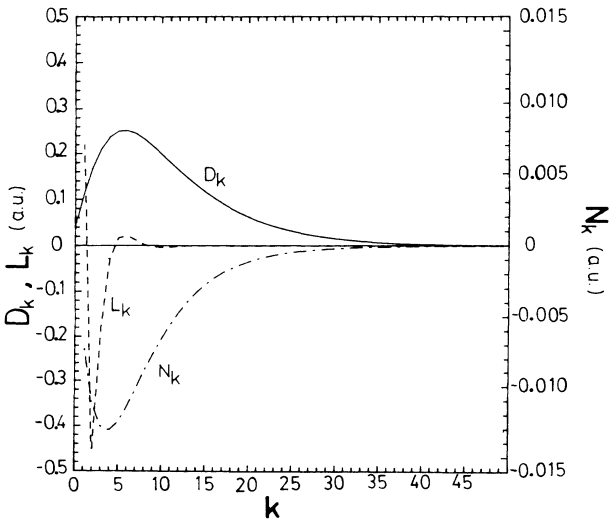

FIG. 3. Coefficients D_k, N_k, and L_k as for Fig. 2: ——, D_k; —·—, N_k; — — —, L_k. The values D_k and L_k are normalized to $\sum_k D_k P_k(\cos\theta)=d\sigma/d\Omega$ in a.u.

where $\phi(l_a,l_b)$ denotes the phase of the scattering matrix

$$S_{l_a l_b}\equiv((L_B l_b)j_t m_t\,|\,S\,|\,(L_A l_a)j_t m_t)\ .$$

In the distorted-wave Born approximation, $\phi(l_a,l_b)$ can be written as a sum of elastic phase shifts with a possible additional term[22] from negative signs of radial overlap integrals,

$$\phi(l_a,l_b)=\delta_{l_a}(E_a)+\delta_{l_b}(E_b)+N_{l_a l_b}\pi\ . \tag{18}$$

For $k=1$ and $\zeta=(l_a-l_b+l_a'-l_b')/2=0$, the value of $|\tau|=(l_a+l_b-l_a'-l_b')/2$ is zero from $|\tau|\le k-|\eta|$. Then $|\tau|=\zeta=0$ yields $l_a=l_b'$ and $l_b=l_a'$, whereby

$$\begin{aligned}\sin[\phi(l_a,l_b)-\phi(l_a',l_b')]=\sin\{&[\delta_{l_a}(E_a)-\delta_{l_a}(E_b)]\\ &+[\delta_{l_b}(E_b)-\delta_{l_b}(E_a)]\\ &+(N_{l_a l_b}-N_{l_b l_a})\pi\}\ .\end{aligned} \tag{19}$$

This expression is very small if the plane shift is a slowly varying function of energy, i.e., when the delay time[23] $[2\hbar\,\partial\delta_l(E)/\partial E]$ is short. N_1 itself is also very small, being a linear combination of dynamical parameters of almost zero magnitudes.

The short-delay-time condition holds when[24]

$$\frac{\Delta E\, l}{E_a\,\Delta l}\ll 1\ , \tag{20}$$

where ΔE is the atomic excitation energy, E_a is the impact energy, and $\Delta l=1$. Therefore it holds at high impact energies and for low partial waves. High partial waves do not change the result $N_1\approx 0$; not only their contribution is small but also $\sin[\phi(l_a,l_b)-\phi(l_a',l_b')]\approx 0$ by another reason, which can be easily checked from the well-known phase-shift formulas for the $1/r^4$ potential for electron-atom collision at large impact parameters.[25]

TABLE III. Coefficients D_k and N_k, with $\eta=0$ and $\zeta=0$ contributions separated for the process (1). Numbers in brackets represent the exponent of the power of ten factors.

k	D_k $(\eta=0)$	D_k $(\zeta=0)$	N_k $(\eta=0)$	N_k $(\zeta=0)$
0	0.369 16[−01]	0.000 00[+00]	0.000 00[+00]	0.000 00[+00]
1	0.100 91[+00]	0.867 96[−03]	−0.667 57[−02]	0.870 02[−04][a]
2	0.152 25[+00]	0.242 61[−02]	−0.878 37[−02]	−0.187 64[−02]
3	0.190 73[+00]	0.266 36[−02]	−0.945 44[−02]	−0.263 92[−02]
4	0.217 15[+00]	0.111 54[−02]	−0.924 56[−02]	−0.300 78[−02]
5	0.233 01[+00]	−0.246 56[−02]	−0.856 77[−02]	−0.306 71[−02]
6	0.240 08[+00]	−0.769 24[−02]	−0.768 21[−02]	−0.291 14[−02]
7	0.240 17[+00]	−0.138 00[−01]	−0.674 40[−02]	−0.263 11[−02]
8	0.234 97[+00]	−0.199 76[−01]	−0.583 83[−02]	−0.229 62[−02]
9	0.225 94[+00]	−0.255 77[−01]	−0.500 72[−02]	−0.195 40[−02]
10	0.214 29[+00]	−0.301 95[−02]	−0.426 72[−02]	−0.163 25[−02]
11	0.201 01[+00]	−0.336 48[−01]	−0.362 08[−02]	−0.134 59[−02]
12	0.186 84[+00]	−0.359 21[−01]	−0.306 13[−02]	−0.109 91[−02]
13	0.172 36[+00]	−0.371 14[−01]	−0.258 61[−02]	−0.891 70[−03]
14	0.158 00[+00]	−0.373 79[−01]	−0.218 03[−02]	−0.720 40[−03]
15	0.144 04[+00]	−0.368 91[−01]	−0.183 66[−02]	−0.680 56[−03]
16	0.130 70[+00]	−0.358 23[−01]	−0.154 61[−02]	−0.467 41[−03]
17	0.118 11[+00]	−0.343 29[−01]	−0.130 10[−02]	−0.376 35[−03]
18	0.106 34[+00]	−0.325 42[−01]	−0.109 46[−02]	−0.303 34[−03]
19	0.954 44[−01]	−0.305 72[−01]	−0.920 80[−03]	−0.244 91[−03]
20	0.854 10[−01]	−0.285 06[−01]	−0.774 61[−03]	−0.198 19[−03]

[a]Note the small value of N_1 $(\zeta=0)$ which derives from the very short delay time for the collision process (1) at 80 eV impact energy.

Next let us examine the influence of the result $N_1(\zeta=0)\approx 0$. Equation (16) for the first two L_1 and L_2 coefficients can be written, neglecting $N_1(\zeta=0)$, as

$$L_1 \approx \frac{-\frac{3}{5}N_2}{2(d\sigma/d\Omega)_{\theta=\pi}}, \quad L_2 \approx \frac{N_2-\frac{4}{7}N_3}{2(d\sigma/d\Omega)_{\theta=\pi}} \quad \text{for } \zeta=0 \tag{21a}$$

$$L_1 \approx \frac{N_1-\frac{3}{5}N_2}{2(d\sigma/d\Omega)_{\theta=\pi}}, \quad L_2 \approx \frac{N_2-\frac{1}{3}N_1-\frac{4}{7}N_3}{2(d\sigma/d\Omega)_{\theta=\pi}} \quad \text{for } \eta=0\ . \tag{21b}$$

Two consequences follow immediately from (21). First, in contrast to N_k where $\eta=0$ components dominate $\zeta=0$, $L_k(\zeta=0)$ for $k=1,2$ will have comparable magnitudes to those of $L_k(\eta=0)$. Second, L_1 and L_2 will have opposite signs for $\zeta=0$, while having the same sign for $\eta=0$, whereby the $\zeta=0$ component may predominate at large angles where P_{11} and P_{21} also have opposite signs. It is obvious from (21a) that L_1 with $\zeta=0$ will have sign opposite that of $N_2(\zeta=0)$. On the other hand, $L_2(\zeta=0)$ will have the same sign as $N_2(\zeta=0)$ because N_3 has a coefficient which is $\frac{4}{7}$ times smaller than that of N_2, if N_k does not vary rapidly as a function of k. A slow variation of N_k with k is expected at intermediate and high energies. Thus opposite signs result for the $\zeta=0$ components of L_1 and L_2. When $\eta=0$, N_1 is not small and then, as for $L_2(\eta=0)$, $L_1(\eta=0)$ will have the same sign as $N_1(\eta=0)$. For $L_2(\eta=0)$, the prediction of the sign does not seem so easy at first glance without solving scattering equations, because of the presence of all three coefficients N_k. But (21b) predicts that $L_2(\eta=0)$ and N_k will have the same sign if the N_k vary linearly with k. This result is not expected to change in practice since N_k is most likely to have a negative second derivative (i.e., convex) at small k before reaching its maximum. Otherwise, the distribution of N_k would be too sharp, yielding a broad angular distribution, which is highly improbable at intermediate and high energies. Since N_k is likely to have the same sign for all k at intermediate and high energies in order for $\langle L_k D_{b\theta}\rangle$ to have a peak at small angles, L_1 and L_2 should also have the same sign. On the other hand, $P_{11}\propto\sin\theta$ and $P_{21}\propto\sin 2\theta$ have opposite signs at $\pi/2<\theta<\pi$ and yield constructive interference if their coefficients L_1 and L_2 are of opposite sign. Thus $\zeta=0$ components may predominate at large angles. The numerical calculation shown in Fig. 4 shows that the predominance of $\zeta=0$ over $\eta=0$ components is quite remarkable for the process (1). Such predominance might, however, depend on system, impact energy, etc.

2. *Importance of only a few partial waves for $\zeta=0$*

We showed in Sec. IV B 1 that $\zeta=0$ components predominate for orientation at large angles. A very good opportunity to identify detailed and specific dynamical information follows from this result, since only a few partial waves participate significantly for $\zeta=0$ components, as shown in Fig. 5, where the convergence of partial sums

$$\sum_{\sigma=k}^{\sigma_c}\sum_{\tau=-k+1}^{k-1}\sum_{\eta\pm 1} L_k(\sigma,\tau,0,\eta) \tag{22}$$

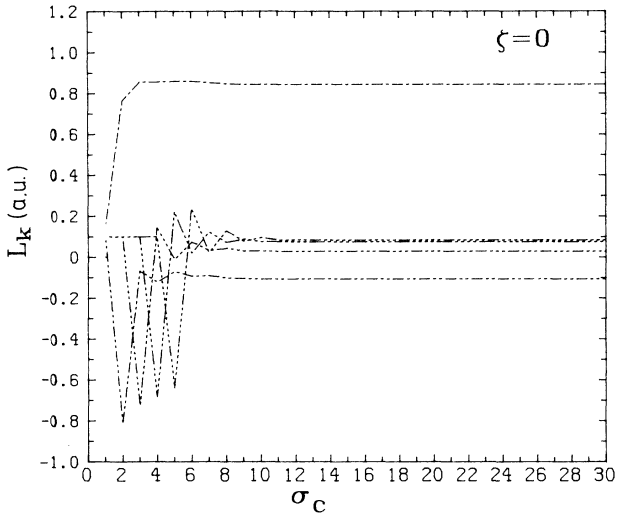

FIG. 5. Truncated sums $\sum_{\sigma=k}^{\sigma_c}\sum_{\tau=-k}^{k}\sum_{\eta}L_k(\sigma,\tau,0,\eta)$ for $k=1$–5 vs σ_c: —·—, $k=1$; —··—, $k=2$; — · · · —, $k=3$; —····—, $k=4$; —·····—, $k=5$.

for $k=1$–5 is plotted as functions of increasing σ_c.

The fast convergence observed in Fig. 5 derives from two causes. In paper II, we showed that large σ (or l) belong to a classically forbidden range for $\zeta=0$. We can tell easily whether a given σ belongs to a classically forbidden range by calculating $\cos\theta$ from

$$\mathbf{j}_t\cdot\mathbf{k}=(\sigma+1)\eta+\tau\zeta\approx(j_t+\tfrac{1}{2})(k+\tfrac{1}{2})\cos\theta\ . \tag{23}$$

If $\cos\theta$ calculated from (23) is larger than unity, the given value of σ belongs to a classically forbidden range. For $k=1$ and $j_t=1$, $\sigma\geq 2$ belongs to a classically forbidden range. Only $\sigma=1$ does not belong to a classically forbidden range. This is one cause for the fast convergence of N_k and thus L_k versus σ. The other cause comes from the existence of Q symmetry in the dynamical parameters (17) for $\zeta=0$ components after a few σ. The possible existence of Q symmetry is expected in the dynamical parameters for $\zeta=0$ components from their very structure, i.e., (parity favored-unfavored)–(parity unfavored-favored). The first and second terms of this expression, differing in the exchange of input and output indices might even cancel out at some σ. Such a cancellation actually occurs for process (1) at 80 eV, accelerating the convergence.

Figure 5 shows that $L_1(\zeta=0)$ already attains 90% of its value with $\sigma=2$ alone. Note that the $\sigma=1$ contribution is quite small due to $N_1(\zeta=0)\approx 0$. Then, from (21), $N_2(\sigma=2)$ is the almost sole source of

$$N_k=\sum_{\sigma=k}^{\infty}\sum_{\tau=-k+1}^{k-1}\sum_{\eta\pm 1}N_k(\sigma,\tau,0,\eta)\ , \tag{24}$$

and contributes to $L_1(\zeta=0)$ through (12). Since $|\tau|\leq k-|\eta|=1$, a unit value of τ contributes to $N_2(\sigma=2)$. Only positive τ is taken here owing to P symmetry as discussed in paper I. These sets of new quantum numbers $(\sigma=2,\ \tau=1,\ \zeta=0,\ \eta=\pm 1)$ correspond to $(l_a,l_b,l_a',l_b')=(2,1,0,1)$ and $(1,2,1,0)$ from (3). Likewise, $N_2(\sigma=2,\ \tau=1)$ and $N_3(\sigma=3,\ \tau=2)$ are identified as contributing to most of $L_2(\zeta=0)$ from Fig. 5. Then, from (16), the orientation formulas can be written down in terms of these $N_k(\sigma,\tau,0,\eta)$ or equivalently of the corresponding dynamical parameters (17) using Eq. (16) and (24) of paper I and of the differential cross section at $\theta=180°$:

$$\begin{aligned}
L_1(\zeta=0)&=\frac{9\sqrt{2}}{80k_a^2}\frac{\mathrm{Im}(S_{21}S_{01}^*-S_{12}S_{10}^*)}{(d\sigma/d\Omega)_{\theta=\pi}}(83\%)+(17\%)\ ,\\
L_2(\zeta=0)&\frac{-\frac{3}{8}\sqrt{2}\,\mathrm{Im}(S_{21}S_{01}^*-S_{12}S_{10}^*)+\frac{1}{7}\sqrt{3}\,\mathrm{Im}(S_{32}S_{01}^*-S_{23}S_{10}^*)}{k_a^2(d\sigma/d\Omega)_{\theta=\pi}}(92\%)+(8\%)\ ,
\end{aligned} \tag{25}$$

where the scattering matrices $S_{l_a l_b}$ are defined just below Eq. (17) and k_a denotes the incident projectile wave number. The second terms in parentheses of L_1 and L_2 are much smaller than the first and can be neglected (see the discussion at the very end of Sec. V B of paper III). The orientation formula at large angles is thus approximated by

$$\langle L_y\rangle_\theta\approx\frac{P_{11}(\cos\theta)\mathrm{Im}[(9\sqrt{2}/80)S_{21}S_{01}^*]+P_2(\cos\theta)\mathrm{Im}\{[-(3\sqrt{2}/8)S_{21}+(\sqrt{3}/7)S_{32}]S_{01}^*\}}{k_a^2(d\sigma/d\Omega)_{\theta=\pi}}\ . \tag{26}$$

3. *Explanation of observations on orientation*

Equation (16) or (26) predicts that the magnitude of orientation will increase as the differential cross section at $\theta=\pi$ decreases in its denominator. It will be interesting to check whether underestimates of the existing theoretical calculations for the magnitudes of orientation at large angles derive from overestimates of the theoretical differential cross sections at large angles.[26]

The shift of the angle of zero orientation (70° for 80 eV) toward a smaller value with increasing impact energy can be explained from the very structure of the formulas for L_k in Eq. (25) or (26). Kelsey[27] obtained the formula for the second Born scattering amplitudes f which are dominant at large angles for the process (1)

$$f(1\,^1S_0\rightarrow 2\,^1P_{1j})\approx\frac{i(1.09)m^2e^4}{q^2p_a}\hat{\mathbf{j}}\cdot(\hat{\mathbf{p}}_a-\hat{\mathbf{p}}_b)\ , \tag{27}$$

where j in P_{1j} and $\hat{\mathbf{j}}$ denote one of the (x,y,z) components of the He $2\,^1P$ state, q denotes the momentum

transfer, p_a and p_b denote the incident and outgoing momenta of the projectile. From (27), the energy dependence of $[k_a^2(d\sigma/d\Omega)_{\theta=\pi}]^{-1}$ is given by E_a^2. Numerical study shows that scattering matrices $S_{l_a l_b}$ increase with increasing impact energy. Thus the modulus of each $\mathrm{Im}(S^\dagger S)/[k_a^2(d\sigma/d\Omega)_{\theta=\pi}]$ increases with increasing energy. The effect of this increase is directly reflected into $L_1(\zeta=0)$ but cancels in $L_2(\zeta=0)$ where two such terms appear with opposite signs, as evident in (25) or (26). For the same reason, the dependence of $L_1(\eta=0)$ and $L_2(\eta=0)$ on energy will be more or less similar to that of $L_2(\zeta=0)$ and thus may not change much as compared to that of $L_1(\zeta=0)$. Since $L_1(\zeta=0)P_{11}(\cos\theta)$ gives a nonnegative contribution (negative in another convention) for all angles, the increase of the modulus of $L_1(\zeta=0)$ while other coefficients remain constant will shift the zero of orientation to smaller angles.

A sudden change of a sign at large angles when $l=2$ is added, observed in Ref. 13, is also easily explained. Note that the orientation given by the approximate equation (25), which applies to large angles and is thus responsible for the change of sign of orientation at large angles, is zero with $l=0$ and 1 partial waves alone. It suddenly acquires its values when the $l=2$ partial wave is included. Inclusion of higher partial waves will not change the result dramatically since (25) receives higher partial-wave contributions only from $l=3$ through the insignificant second term N_3 of (21a). The exclusion of $l=0$ and 1 partial waves in (25) derives from $N_1(\zeta=0)\approx 0$(short delay time). The lowest partial wave contribution to N_2 enters through $S_{21}S_{01}^*$, as explained below (24).

Also Eq. (25) or (26) clearly shows which factors are responsible for the sign of the orientation at large angles. Note first that another systematics discussed at the end of Sec. V B instead of propensity rules for $\eta=0$ components applies to the dynamical parameters in (25). This is utilized to simplify (25) into (26). Secondly, S_{01}^* factors out in the approximate formula (26)

$$\langle L_y \rangle_\theta \propto \mathrm{Im}[(9\sqrt{2}P_{11}S_{21}/80+P_{21}\cdots)S_{01}^*] , \qquad (28)$$

which does not correspond to the propensity favored terms. Influence of the correction term $N_{l_a l_b}\pi$ in (18) is therefore likely actually to occur in the process (1), making the sign of orientation positive (or negative in the other convention). The negative radial overlap integral responsible for the correction term implies the significance of a negative transition charge density in this particular process, which is normal in positron-atom collisions.

Accordingly, the sign of the orientation at large angles depends on three causes: the predominance of $\zeta=0$ components, systematics on the predominance of $\mathrm{Im}(S_{l_a l_b}S_{l_a' l_b'}^*)$ or $\mathrm{Im}(S_{l_b l_a}S_{l_b' l_a'}^*)$ (different Q parity terms), and the occurrence of the negative radial overlap integrals.

4. *Further consequences of $\eta=0$ and $\zeta=0$ separation*

The separation of $\zeta=0$ and $\eta=0$ components makes it easy to predict the sign of orientation at small angles. This prediction would be difficult for $\zeta=0$ components which have the dynamical parameters of the form (parity favored-unfavored)–(parity unfavored-favored), without solving scattering equations. It is instead easy for the $\eta=0$ components with the form (parity favored-favored)–(parity unfavored-unfavored), where the first term is clearly bigger than the second. The predominance of the $\eta=0$ components at small angles settles the controversy described in the third paragraph of the Introduction. Detailed discussions on this and the connection between the classical rolling-ball model and quantum formulas are given in Ref. 17.

V. DISCUSSION

The approximate formula (25) or (26) can explain most observations on orientation. This study demonstrates that electron-photon coincidence experiments on process (1) provide a rare opportunity to obtain information on the dynamical parameters with $\zeta=0$. For the differential cross section, the same analysis shows that $\eta=0$ components predominate at both small and large angles. However, some problems are not solved yet.

The plot of partial sums

$$\sum_{\sigma=k+1}^{\sigma_c}\sum_{\tau=-k}^{k}\sum_{\zeta=\pm 1} L_k(\sigma,\tau,\zeta,0) , \qquad (29)$$

as functions of increasing σ_c, reveals sharp oscillations of L_k from one value of σ_c to the next in Fig. 6. The origin of this phenomenon lies in the contribution of the sums over σ in (29) for the N_k in large parentheses in (16) where successive terms have coefficients of opposite sign. Since the sum over σ runs only over positive values of $\sigma-\tau-\zeta$, each stepwise increase of σ_c contributes to L_k a term of alternating sign. This oscillation in L_k implies extensive cancellations in Eq. (29). Attempts to identify the surviving significant dynamical terms important for

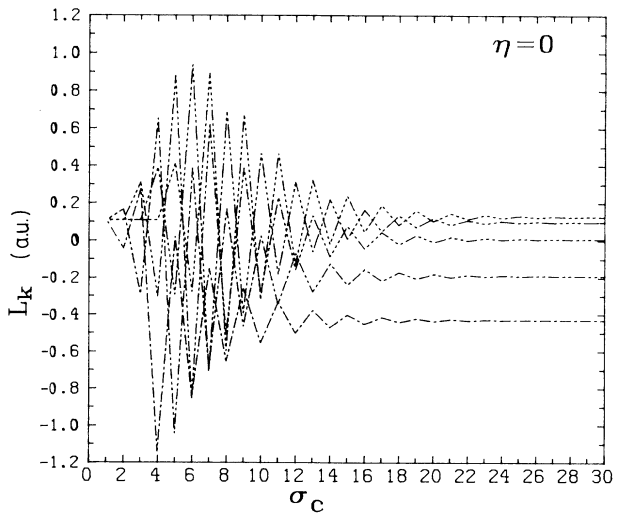

FIG. 6. Truncated sums $\sum_{\sigma=k+1}^{\sigma_c}\sum_{\tau=-k+1}^{k-1}\sum_{\zeta=\pm 1}\times L_k(\sigma,\tau,\zeta,0)$ for $k=1$–5 vs σ_c: —·—, $k=1$; —··—, $k=2$; — · · · —, $k=3$; —·····—, $k=4$; —·····—, $k=5$.

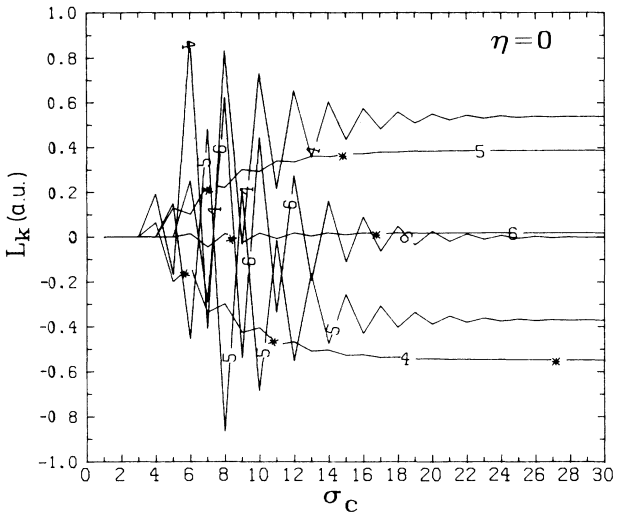

FIG. 7. Separation of the contributions $\sum_{\tau=0}^{\tau\leq k/2}$ (without asterisk) and $\sum_{\tau\geq k/2}^{k}$ (with asterisk) for $\eta=0$, $k=4,5,6$.

the orientation at small scattering angles have not been successful. A study on the cancellation of the first Born amplitudes that commonly appear both in $\langle L_y D_{b\theta}\rangle$ and $\langle D_{b\theta}\rangle$ as dominant contributions at small angles may prove useful to solve this problem.

Separate contribution from larger and smaller values of $|\tau|/(k-|\eta|)$ are plotted in Fig. 7 by sorting out the contributions to L_k as functions of σ_c from $|\tau| \gtrless (k-|\eta|)/2$. In Fig. 7, the oscillations discussed above are prominent only for large $|\tau|$. More importantly, the contributions from larger and smaller τ have comparable magnitude and opposite signs, thus contributing to the generally faster convergence of L_k to zero for larger k. The origin of this cancellation remains to be solved.

Final comment concerns the inversion problem, i.e., the problem of extracting dynamical parameters for experimental data. It is well known in the elastic scattering theory that most details of wave functions and potentials at short ranges do not appear in scattering observation. The shift of the phase of a wave function from that of a wave function for zero potential scattering suffices to determine observation in asymptotic regions. Or, inversely, phase shifts and eventually potentials can be extracted from the scattering experiments. The inversion problem in the literature usually refers to obtaining potentials from the phase shifts that are assumed to be known. This may be true for elastic scattering. However, for inelastic scattering it is not trivial even to extract the corresponding phase shifts, i.e., short-range dynamical parameters or quantum-eigendefects.[28] In this paper, the most significant dynamical parameters are identified at large scattering angles, from which it might be possible to extract short-range dynamical parameters by the theory developed in Ref. 29 modified for application to an electron-atom scattering system. Eventually, this procedure may prove important.

ACKNOWLEDGMENTS

This work was supported by the U.S. Department of Energy, Division of Basic Chemical Sciences and submitted to the Department of Chemistry of the University of Chicago in partial fulfillment of requirements for a Ph.D. degree. I am greatly indebted to Professor U. Fano for the guidance, the great help in the preparation of the manuscript, and a lot of insightful comments. The present form of some parts, especially Sec. II, of the paper is due to Professor J. C. Light. I would like to thank Dr. D. H. Madison for sending me the results of DWBA calculations and for several technical but important comments to the work. Dr. N. Andersen's encouraging comments and his making available unpublished manuscripts are also greatly acknowledged. I would like to thank Dr. J. Callaway for sending me the phase-shift data for the process (1).

APPENDIX A: CHARACTERISTICS OF HARMONIC EXPANSIONS

Expansions of angular distributions into Legendre polynomials $P_k(\cos\theta)$ and their associated functions $P_{k1}=dP_k(\cos\theta)/d\theta$ are analogous to Fourier expansions in their density of the relations of the type $\Delta k\,\Delta\theta\approx 1$. These relations connect the width $\Delta\theta$ of a peak or the wavelength of oscillation of an angular distribution $f(\theta)$ to the spectral width Δk of corresponding coefficients f_k.

Another characteristic of harmonic expansion proves important to tell how wide and sharp (narrow) harmonic distributions are from the oscillation period of angular measurements. If the distribution of harmonic coefficients has, e.g., a square shape of width Δk, the corresponding angular distribution has a period $2\pi/\Delta k$ which also equals the position of its first minimum. (Peaks of angular distribution at zero degree seem to break the periodicity but result from a singularity.) A smoother distribution in k with the same width narrows the ratio of peaks to troughs of $f(\theta)$ but leaves its period of oscillation unchanged.

The differential cross section $\langle D_{b\theta}\rangle$ for the process (1) at 80 eV has a forward peak of half-width 8°;[30] the corresponding distribution of D_k peaks at $k=7$ with a standard deviation $\Delta k\approx 7$ (see Table I). On the other hand, the distribution of $\langle L_y D_{b\theta}\rangle$ starts at zero at $\theta=0$, then peaks and returns to zero at 70°, with a standard deviation 5.8 of N_k (Table I) approximately equal to $360°/70°\approx 5.15$, as calculated from the formula $2\pi/\Delta k$. [A zero of $\sum_k N_k P_{k1}=d(\sum_k N_k P_k)/d\theta$ corresponds to an extremum, the first minimum in this case, of $\sum_k N_k P_k$.]

APPENDIX B: U MATRIX

The characteristic forward peak of differential cross sections at intermediate and high energies greatly reduces the dimension of the U matrix required to attain the reasonably good value of the matrix elements $(U^{-1})_{mn}$ with small m and n.

The sharp decrease ($\Delta\theta\approx 8°$) of the differential cross section $\langle D_{b\theta}\rangle$ from its value at $\theta=0$ produces a very

sharp peak at an angle less than 8° in the integrand of Eq. (9) when multiplied by the sharp increase of $P_{n1}(\cos\theta)$ ($m \leq n$) of (9). The largest contribution to the integral (9) comes then from the narrow range of angles around the peak at near zero degree. In this range, $P_{m1}(\cos\theta)$ can be approximated by

$$P_{m1}(\cos\theta) \approx -\tfrac{1}{2}m(m+1)P_{11}(\cos\theta) , \quad \text{(B1)}$$

whereby we obtain

$$U_{mn} = \tfrac{1}{2}m(m+1)U_{1n} \quad (m \leq n) . \quad \text{(B2)}$$

Numerical study shows that if the relation (B2) holds among U matrix elements, the matrix elements $(U^{-1})_{mn}$ obtained from a submatrix of U with dimension m are almost the same as those obtained from a larger submatrix; m can be as small as 2. [This reasonable property derived easily from (B2).]

Equation (9) implies that the $n \times n$ submatrix of U can be obtained from D_k values with $k \leq 2n$. Thus if a submatrix smaller than 5×5 is enough for orientation, as is the case at large angles as described in Sec. III, only D_k values with k less than 10 need be included.

*Present address: 127-72, Chemistry, California Institute of Technology, Pasadena, CA 91125.

[1]C. W. Lee and U. Fano, Phys. Rev. A **33**, 921 (1986).
[2]C. W. Lee, Phys. Rev. A **34**, 959 (1986).
[3]C. W. Lee and U. Fano, Phys. Rev. A **36**, 66 (1987).
[4]C. W. Lee and U. Fano, Phys. Rev. A **36**, 74 (1987).
[5]M. Eminyan, K. B. MacAdam, J. Slevin, M. C. S. Standage, and H. Kleinpoppen, Phys. Rev. Lett. **31**, 576 (1972).
[6]N. Andersen and I. V. Hertel, Comments At. Mol. Phys. (to be published).
[7]G. Csanak, in *International Symposium on Correlation and Polarization in Electronic and Atomic Collisions,* edited by A. Crowe (World Scientific, Singapore, 1988).
[8]M. Kohmoto and U. Fano, J. Phys. B **14**, L447 (1981).
[9]H. W. Hermann and I. V. Hertel, J. Phys. B **13**, 4285 (1980).
[10]J. Slevin, Rep. Prog. Phys. **47**, 461 (1984).
[11]I. V. Hertel, H. Schmidt, A. Bäring, and E. Meyer, Rep. Prog. Phys. **48**, 375 (1985).
[12]D. H. Madison and K. H. Winters, Phys. Rev. Lett. **47**, 1885 (1981).
[13]D. H. Madison, G. Csanak, and D. C. Cartwright, J. Phys. B **19**, 3361 (1986).
[14]U. Fano and J. H. Macek, Rev. Mod. Phys. **45**, 553 (1973).
[15]U. Fano, Rev. Mod. Phys. **29**, 74 (1957).
[16]G. Gabrielse, Phys. Rev. A **22**, 138 (1980).
[17]C. W. Lee, in *International Symposium on Correlation and Polarization in Electronic and Atomic Collisions,* edited by A. Crowe (World Scientific, Singapore, 1988).
[18]In the study of alignment, different values of k_a and k_b appear in the summation and thus k in the harmonic expansion is no longer equal to k_a and k_b. Thus k_a and k_b themselves are not directly related to observables. Complications in the use of P and Q symmetries may be expected from this.
[19]D. H. Madison and W. N. Shelton, Phys. Rev. A **7**, 499 (1973); D. H. Madison and K. H. Winters, J. Phys. B **16**, 4437 (1983).
[20]Dr. Inokuti informed me that Eq. (14) may be a quite general characteristic of intermediate energy collisions (see Ref. 17 for more details).
[21]L. Schiff, *Quantum Mechanics* (McGraw-Hill, New York, 1955).
[22]I am indebted to Dr. D. H. Madison for this: The radial overlap integral, appearing in the first DWBA, is defined as the integration of a transition potential sandwiched between initial and final distorted waves, both of which are assumed positive near the origin: the transition potential represents $(\psi_b \mid V \mid \psi_a)$, where ψ_a and ψ_b denote the initial and final target states and V the potential between target and projectile and where the integration is performed only over target coordinates.
[23]F. T. Smith, J. Chem. Phys. **42**, 2419 (1965).
[24]C. W. Lee, Ph.D. thesis, The University of Chicago, 1987 (unpublished).
[25]N. A. W. Holzwarth, J. Math. Phys. **14**, 191 (1973).
[26]See, e.g., N. Andersen and I. V. Hertel, Ref. 6.
[27]E. J. Kelsey, Phys. Rev. A **14**, 56 (1976).
[28]U. Fano and A. R. P. Rau, *Atomic Collisions and Spectra* (Academic, New York, 1986); U. Fano, Phys. Rev. A **2**, 353 (1970).
[29]E. S. Chang and U. Fano, Phys. Rev. A **6**, 173 (1972).
[30]C. B. Opal and E. C. Beaty, J. Phys. B **5**, 627 (1972).